Percolation of water in aqueous solution and liquid–liquid immiscibility

A. Oleinikova, I. Brovchenko, and A. Geiger
Physikalische Chemie, Universität Dortmund, 44221 Dortmund, Germany

B. Guillot
Laboratoire de Physique Theorique des Liquides, Universite P.&M. Curie, 75252, Paris, France

(Received 2 April 2002; accepted 21 May 2002)

The first simulation study of the percolation of hydrogen bonded water clusters in the vicinity of the region of immiscibility of an aqueous solution (of tetrahydrofuran) is reported. Percolation of water is found in a wide concentration range on both sides of the liquid–liquid coexistence curve. An infinite cluster appears with a probability of 50% at a water fraction significantly lower than the one corresponding to the organic-rich branch of the coexistence curve. The fractal dimension d_f of the infinite clusters at this threshold is found close to the two-dimensional (2D) value, $d_f(2D) \cong 1.9$. Three-dimensional (3D) percolation clusters form at the organic-rich branch of the coexistence curve. At this water concentration the fractal dimension of an infinite cluster reaches the 3D value $d_f(3D) \cong 2.5$ and the cluster size distribution follows a power law with an exponent $\tau \cong 2.2$. The analysis of the clustering of the organic (tetrahydrofuran) molecules indicates that the immiscibility gap of an aqueous solution corresponds to the concentration interval where both components are above their respective percolation threshold. © *2002 American Institute of Physics.*
[DOI: 10.1063/1.1493183]

I. INTRODUCTION

The relation between the macroscopic properties of a fluid and its microscopic structure—described in terms of molecular clusters—is an old problem originating from Mayer's theory,[1] and is still an area of active researches.[2] Fisher made use of clusters of particles in his phenomenological theory of condensation.[3] The development of percolation theory provoked studies of a possible correspondence between percolation transitions and the thermodynamic critical point in lattice models. It was found for the Ising model that the percolation transition could be mapped on the critical point, if a purely geometrical definition of clusters is replaced by a special physical (energetic) definition of bonded pairs.[4]

There is no unambiguous criterion of particle connectivity in simple continuum models.[5] But also in this case, using a proper definition of clusters, the percolation line can meet the coexistence curve at the critical point.[6,7] Above the critical temperature a transition from a system composed of finite clusters to an infinite percolating network of particles can be expected at some density. In particular, a line, corresponding to the vanishing surface tension of droplets, the so-called Kertezh line, was predicted.[8] But despite all efforts, the relation between percolation and thermal behavior is still not clear, even for spin systems.[9] For fluid systems computer simulations revealed the existence of a percolation transition in the supercritical state of Lennard-Jones (LJ) fluids[10,11] and water.[12–17] However, the actual location of a percolation line at supercritical temperatures is strongly dependent on the definition of clusters.

Recently Campi *et al.* studied the percolation behavior of a lattice gas model using a definition of droplets based on an energetic stability criterion.[18] A percolation line, which joins the thermodynamic critical point to the critical point of bond percolation, was found. Along this line, the droplet size distribution n_s, with s being the cluster size, follows a power law $n_s \sim s^{-\tau}$ with an exponent $\tau \cong 2.2$ valid for random percolation.[19,20] A similar percolation line is found in LJ fluids, if the cluster definition is based on a bond criterion which includes relative kinetic energy of pairs.[11]

Much less is known about the relationship between percolation loci and first-order phase transitions. Early investigations suggested that below the critical temperature phase separation occurs before an infinite cluster could appear in the system. This means that a true percolation transition would not be observable in stable and probably not even in metastable regions. Klein suggested that the occurence of infinite ramified droplets gives rise to a spinodal line, which is a line of percolation transitions,[21] while the cluster distribution has only a weak singularity at the coexistence curve. More recently it was shown however, that the Ising model, mapped on the Bethe lattice, allows the simultaneous presence of two infinite percolating clusters of opposite spins in the metastable region.[22]

For realistic systems with short-range interactions the spinodal curve is not well defined. In systems with finite-range interactions a spinodal line as well as spinodal singularities should be rounded.[23–25] Inside the two-phase coexistence region a percolation is a transient phenomenon, therefore, there are many possible ways to define a percolation line in this regime.[25]

The relation between phase transition and percolation has become of special importance with recent developments in the analysis of multifragmentation processes in nuclear physics.[26,27] The distribution of nuclear clusters resulting from the decomposition of excited nuclear matter, can be

 © 2002 American Institute of Physics

Downloaded 07 Oct 2004 to 129.217.216.20. Redistribution subject to AIP license or copyright, see http://jcp.aip.org/jcp/copyright.jsp

measured experimentally and therefore provides information about the thermodynamic state of the excited nucleus (a kind of liquid–vapor phase transition of nuclear matter). This problem caused a renewed interest for the possibility to map clustering on thermodynamics, i.e., to relate the cluster size distribution with liquid–vapor (or fluid–fluid) phase transitions.[28–31] The first-order liquid–gas phase transition in small systems was studied in Ref. 28 by means of lattice gas models. It was found that the crossing of the coexistence line is accompanied by a minimum of the effective exponent τ of the cluster size distribution and the occurrence of a prominent maximum of its second moment. The liquid–gas phase transition in a two-component lattice gas model with open boundary conditions could be identified by a local minimum of the exponent τ. Furthermore, a global minimum $\tau=2.2$ is observed in the vicinity of the critical point.[29] Qualitatively similar results were obtained for a microcanonical lattice gas model with fluctuating volume.[30] A power law behavior of the fragment size distribution with an exponent slightly higher than $\tau=2.3$ is observed in the region where a first-order phase transition could be expected.

Despite the numerous simulation studies of the percolation of physical clusters in the various lattice models undergoing first-order phase transition, only one such study has been performed for a continuous model, namely for LJ fluids. Campi *et al.* observed a curve of percolation loci at supercritical temperatures and densities.[11] This percolation curve ends at the thermodynamic critical point. At subcritical densities ($\rho<\rho_c$) or subcritical temperatures ($T<T_c$) no signal of percolation behavior was observed. The cluster distribution n_s deviates from a power law form and decreases much faster with s than $n_s\sim s^{-2.2}$ as it is expected at the true percolation threshold. However, a ''macroscopic'' cluster appears as soon as one penetrates into the two-phase region. This sharp signal corresponds to the crossing of the coexistence curve and could provide a method to determine the liquid–gas phase boundary.

Hydrogen-bonded liquids, such as water, provide a rather well-defined criterion of connectivity, based on the existence of a hydrogen bond between molecules. Therefore, water was one of the first continuous systems used for comprehensive studies of percolation behavior.[32–34] Simulation of the liquid–vapor coexistence curve of water[35] indicates that at the critical point the number of the hydrogen bonds per molecule is equal to the one obtained for the bond percolation threshold of water.[34]

The breakdown of the three-dimensional water network with increasing concentration of solute in aqueous solutions, which are fully miscible over the whole concentration range, is an area of active experimental research.[36–47] Studies of the 1,4-dioxane-water mixture by various experimental methods evidence a breakdown of the water hydrogen-bond network at a 1,4-dioxane mole fraction of about 0.1 (Refs. 36 and 37) to 0.2 (Refs. 38 and 39). In aqueous solution of acetonitrile the infinite water network breaks at about 0.4 mole fraction of acetonitrile.[40,41] Systematic experimental studies of alcohol–water mixtures show that water percolation is no longer present above 0.17, 0.10, and 0.09 mole fractions of methanol,[43(a)] ethanol,[43(b)] and propanol,[43(c)] respectively.

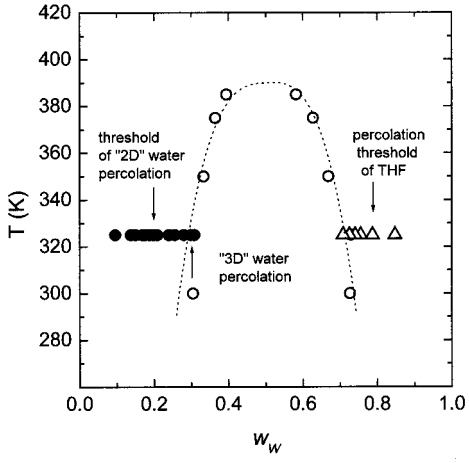

FIG. 1. Liquid–liquid coexistence curve of the aqueous solution of THF in terms of water mass fraction w_W: results of Gibbs ensemble simulations (Ref. 49) (open circles), two-terms fit with critical exponent $\beta=0.33$ and linear diameter (dotted line). Percolation of water at $T=325$ K was studied in 14 organic-rich solutions (solid circles) and percolation of THF in six water-rich solutions (triangles). The liquid–liquid coexistence curve lies in the region where both components of the solution are above their percolation thresholds (indicated by arrows).

The breakdown of the water network in aqueous solutions was also used to explain peculiarities of various thermodynamic properties below 0.1 to 0.2 mole fraction of solutes.[45,46] Finally, recent electrical conductivity measurements in isobutyric acid+water mixtures above the liquid–liquid critical temperature indicate that a percolation line starts at the critical point and remains at the critical composition in some temperature interval.[47]

There are no detailed computer simulation studies of the percolation threshold in aqueous solutions, although an analysis of water clustering is available for some systems.[48] Obtaining a reliable statistics of large and spanning clusters is very time consuming. Another problem is related to the knowledge of the intermolecular potentials, which must correctly reproduce the properties of aqueous solutions in a wide concentration range. As a matter of fact, a high sensitivity of the phase behavior of aqueous solution to slight variations of cross interactions between the solute and the solvent is observed.[49]

In the present paper we report the first study of water percolation in aqueous solution in the vicinity of the region of immiscibility. This study follows the recent simulations of the liquid–liquid coexistence curve of the tetrahydrofuran (THF)+water mixture,[49] shown in Fig. 1. This mixture possesses a closed loop immiscibility gap, which shows a large sensitivity to small changes in experimental conditions, such as deuteration of water or addition of ionic impurities.[50,51] Moreover, the partial substitution of THF by deuterated THF results in a complete disappearance of the immiscibility region.[52] It is recognized, that clustering phenomena play an important role in the evolution of the immiscibility gap in the presently investigated mixture, as in other aqueous solutions.[53,54] So the THF+water mixture is a good candidate to investigate more quantitatively the relation between phase transition and percolation threshold in real liquids.

Downloaded 07 Oct 2004 to 129.217.216.20. Redistribution subject to AIP license or copyright, see http://jcp.aip.org/jcp/copyright.jsp

TABLE I. Parameters of the simulated mixtures at $T=325$ K and results of percolation analysis of water (mixtures 1–14) and THF (mixtures 15–20). x_{THF} and w_{THF} are the mole and mass fractions of THF, N_{THF} and N_W are the numbers of THF and water molecules in the periodic simulation box, respectively. N_{conf} is the number of configurations where a percolation analysis was performed, ρ is the mass density of mixtures, P is the percolation probability, n_{bond} is the average number of bonds between the considered molecules of the same kind ($n_{bond}=n_H$ for water), R is the probability to find an infinite cluster, S_{mean} is the mean cluster size, and d_f is the fractal dimension of the infinite cluster. The size of box was 26.5 ± 0.5 A for mixtures 1–14 and 40.17 ± 0.02 A for mixtures 15–20. Concentrations of the coexisting phases are marked by asterisk.

	x_{THF}	w_{THF}	N_{THF}	N_W	N_{conf}	ρ (g cm^{-3})	P	n_{bond}	R	S_{mean}	d_f
1	0.359	0.692	97	173	1×10^5	0.9071	0.872	2.241	1	8.79	2.602
2*	0.370	0.702	100	170	2×10^5	0.9043	0.841	2.228	0.9992	12.65	2.506
3	0.391	0.720	102	159	2×10^5	0.9003	0.800	2.181	0.9971	13.46	2.410
4	0.421	0.744	106	146	2×10^5	0.8972	0.680	2.089	0.9825	15.97	2.269
5	0.442	0.761	106	134	2.5×10^5	0.8941	0.675	2.055	0.9701	12.29	2.199
6	0.486	0.791	107	113	3×10^5	0.8881	0.598	1.935	0.8005	10.07	2.040
7	0.502	0.801	103	102	2×10^5	0.8869	0.520	1.847	0.7668	8.28	1.943
8	0.520	0.813	105	97	3×10^5	0.8856	0.441	1.755	0.4822	8.76	1.821
9	0.538	0.823	107	92	2×10^5	0.8824	0.488	1.799	0.4967	8.99	1.799
10	0.543	0.826	108	91	3×10^5	0.8817	0.418	1.726	0.3970	8.44	1.737
11	0.551	0.831	113	92	1×10^5	0.8817	0.395	1.660	0.3114	7.25	1.712
12	0.585	0.849	120	85	1×10^5	0.8778	0.439	1.559	0.2190	5.75	1.729
13	0.610	0.862	125	80	2×10^5	0.8763	0.444	1.520	0.0773	5.21	1.651
14	0.703	0.904	130	55	1×10^5	0.8645	0.388	1.228	0.0031	3.25	1.465
15	0.0430	0.152	80	1800	1×10^5	0.976 66	0.205	1.437	0.0064	4.03	1.622
16	0.0633	0.213	112	1656	3×10^5	0.969 27	0.416	2.042	0.5907	10.40	2.289
17	0.0748	0.245	128	1584	3×10^5	0.965 84	0.559	2.518	0.9187	13.38	2.518
18	0.0806	0.260	136	1552	3×10^5	0.965 31	0.626	2.505	0.9779	15.73	2.692
19*	0.0865	0.275	144	1520	3×10^5	0.964 35	0.861	2.755	0.9999	16.11	2.844
20	0.0931	0.291	152	1480	1×10^5	0.961 61	0.932	2.942	1	14.11	2.945

II. METHODS

Monte Carlo (MC) simulations of THF+water solutions were performed in the NPT ensemble at $P=1$ bar and $T=325$ K, 350 K, and 375 K, respectively. The solutions were prepared from different initial configurations and several millions of MC steps were performed for equilibration. Analysis of clusters was carried out every 1000 MC steps. The final results were averaged over 100 000 to 300 000 analyzed configurations.

The intermolecular potentials are the same as those used in the previous study to obtain the liquid–liquid coexistence curve[49] shown in Fig. 1. Water–water interactions are modeled by the TIP4P model of water[55] while THF–THF interaction are handled by a five-site model.[56] For the LJ parameters between unlike species the Lorentz–Berthelot rules are used with a spherical cutoff put equal to 8 A. The Coulombic interactions between THF and water molecules are multiplied by a factor of 1.2 in order to better reproduce the experimental coexistence curve (see Ref. 49).

We have checked the accuracy of these intermolecular potentials to predict the solution density, which is of great importance for percolation study. The simulated densities of 20 THF+water solutions at $T=325$ K are presented in Table I and are compared with available experimental data at $T=328$ K (Fig. 2). It is clear that the chosen intermolecular potentials reproduce the solution density with good accuracy. Uncorrected coulombic interactions between THF and water molecules were used in a MC simulation of THF+water solutions at $T=298$ K in Ref. 57. The densities from this study are found significantly below the experimental data available at the same temperature. This evidences that cross interactions used in the above paper are underestimated. Furthermore, the scattering of the simulated densities observed in the intermediate concentration range probably originates from a liquid–liquid phase separation inside the simulation box of Ref. 57, As a matter of fact use of uncorrected THF-water interactions favors unmixing (see Ref. 49).

Our definition of water connectivity is based on the H-bond criteria adopted for the analysis of percolation in water.[33,34] In this framework two water molecules are considered to belong to the same cluster if they are connected by a continuous H-bond network. A combined energy-distance

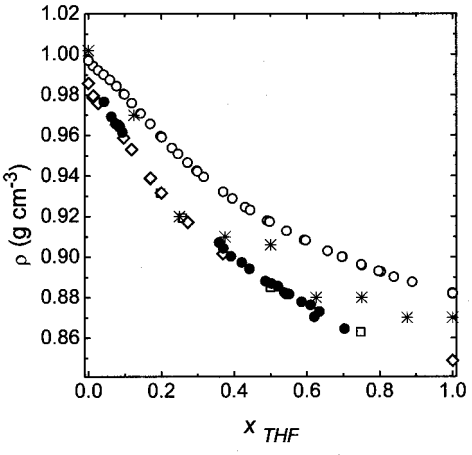

FIG. 2. Densities of the aqueous solutions of THF. Densities at $T=325$ K, obtained in this study (solid circles) with the intermolecular potentials used in Ref. 49. Experimental data at $T=328$ K from Ref. 58 (squares) and Ref. 59 (diamonds). Densities at $T=298$ K, simulated in Ref. 57 (asterisks) with uncorrected cross parameters (see text), and experimental data at the same temperature from Refs. 58–60 (open circles).

Downloaded 07 Oct 2004 to 129.217.216.20. Redistribution subject to AIP license or copyright, see http://jcp.aip.org/jcp/copyright.jsp

H-bond criterion was used to determine the connectivity between water molecules for all studied concentrations and temperatures. This connectivity criterion is much less ambiguous for hydrogen bonds than in the case of LJ models. The value of the H-bond distance $R_W < 3.5$ A is found from the first minimum of the oxygen–oxygen distribution function, while the energetic criterion $U_W < -2.6$ kcal/mol is found from the distribution of the water–water pair interaction energies in solution. The location of the minimum in the latter distribution varies only slightly in the range of temperature and concentration investigated here. These criteria are commonly used for the analysis of hydrogen bonds in computer simulations of water[12–17,35] and lead to an average number n_H of hydrogen bonds per molecule in pure water ($n_H = 3.26$ at $T = 300$ K and $n_H = 3.13$ at $T = 325$ K) which is in agreement with available experimental data (see Ref. 61 for comparison of some experimental and simulation data). The influence of the above connectivity criteria on the cluster distribution is evaluated later in this paper.

Each selected configuration was inspected with the intention to locate the possible presence of an ''infinite'' cluster, i.e., a cluster which spans the periodic simulation box at least in one direction. To identify the percolation threshold we used the following criteria: (i) the probability R to find an infinite cluster is 50%; (ii) the cluster number distribution n_s obeys a power law $n_s \sim s^{-\tau}$ with the universal exponent $\tau = 2.19$,[19] where s is the number of molecules in the cluster; (iii) the infinite cluster at the threshold is a fractal object with fractal dimension $d_f = 2.53$;[20] (iv) the mean cluster size $S_{\text{mean}} = \Sigma n_s s^2 / \Sigma n_s s$ (the largest cluster is excluded from the sums) has a maximum at the threshold in an infinite system or just before the threshold in a finite box. Moreover we calculated the probability P for a given molecule to be a member of the infinite cluster (percolation probability).

The system approaches to the percolation threshold with increasing parameter p, which is a site occupancy for site percolation or a bond probability for bond percolation. It is not clear *a priori* how to choose the parameter p in fluid mixtures to analyze the percolation of components. In simple continuous models the volume and packing fraction are usually used as relevant variables. However, the volume fraction of components is not easy to define in solution with large mixing volume such as THF+water. Therefore, in the present paper we use various concentration variables: w_i, the mass fraction, φ_i, the volume fraction computed in neglecting the mixing volume, x_i, the mole fraction as well as ρ_i, the partial density, where i denotes water or THF.

III. RESULTS

Water clustering is analyzed at fixed temperatures for different water concentrations on both sides of the immiscibility region. The parameters of the investigated solutions and the main results of the percolation analysis are presented in Table I (mixtures 1–14 for the THF-rich side and mixtures 15–20 for the water-rich side). In the one-phase region between the water-rich branch of the coexistence curve and the pure water we found that water in solution always percolates. On the THF-rich side of the coexistence curve water clustering was investigated at $T = 325$ K in solutions of various concentrations including the concentration at coexistence and one concentration in the metastable region (see Fig. 1).

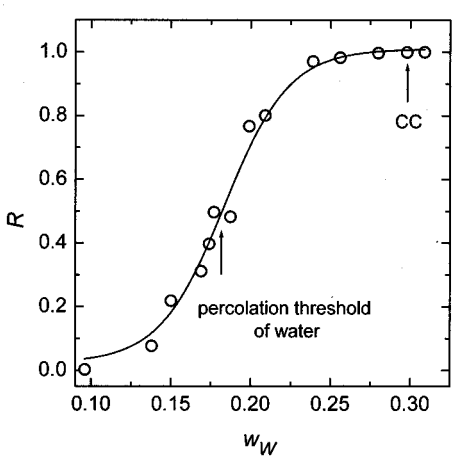

FIG. 3. Probability to find a percolating cluster of water molecules as a function of mass fraction w_W of water in solution (open circles). The fit of the simulation data to a sigmoid function locates a percolation threshold at about $w_W = 0.183$ (arrow). The concentration at the organic-rich branch of the coexistence curve is also indicated (CC) by arrow.

The probability R to find an infinite cluster as a function of the mass fraction of water is given in Fig. 3. The percolation threshold is found at $w_W = 0.183$ ($x_W = 0.473, \varphi_W = 0.162, \rho_W = 0.162$ g cm^{-3}) located far from the organic-rich branch of the coexistence curve at this temperature ($w_{W,CC} = 0.298$, $x_{W,CC} = 0.641$, $\varphi_{W,CC} = 0.269, \rho_{W,CC} = 0.270$ g cm^{-3}). The evolution of the cluster size distribution when crossing this percolation threshold is shown in Fig. 4. At the percolation threshold in the range of cluster

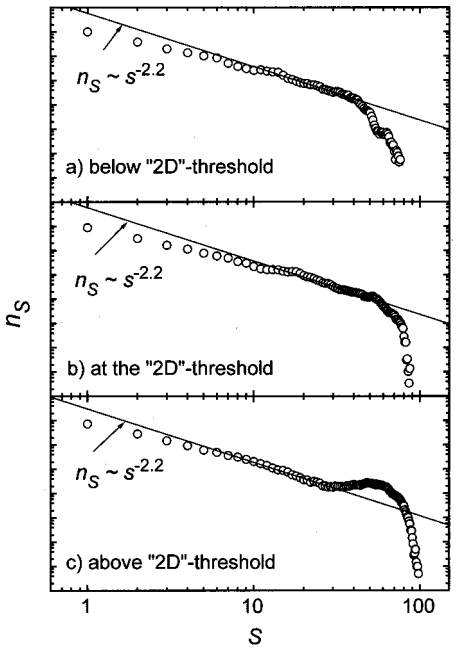

FIG. 4. Size distribution of water clusters in three solutions close to the 2D percolation threshold: (a) $w_W = 0.169$ (below threshold), (b) $w_W = 0.187$ (approximately at the threshold), and (c) $w_W = 0.199$ (above threshold). Scaling law, predicted at the percolation threshold for an infinite 3D lattice, is shown by lines.

Downloaded 07 Oct 2004 to 129.217.216.20. Redistribution subject to AIP license or copyright, see http://jcp.aip.org/jcp/copyright.jsp

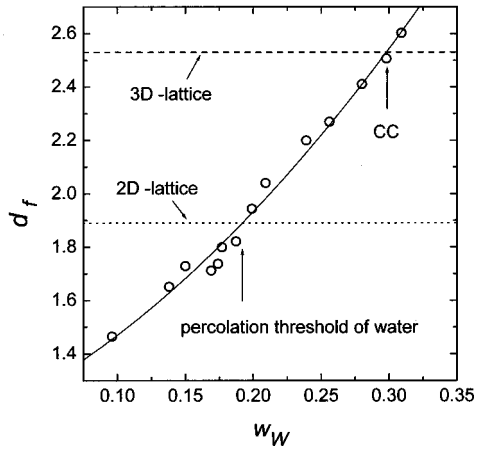

FIG. 5. Fractal dimension d_f of spanning water clusters as function of mass fraction of water (circles) and a polynomial fit (solid line). The exact result for a 2D lattice [$d_f = 91/48$ (Ref. 18)] and $d_f = 2.53$ obtained from recent simulations of a 3D lattice (Ref. 19) are shown by dotted and dashed lines, respectively. The percolation threshold of water in the organic-rich phase and the location of the coexistence curve are indicated by arrows.

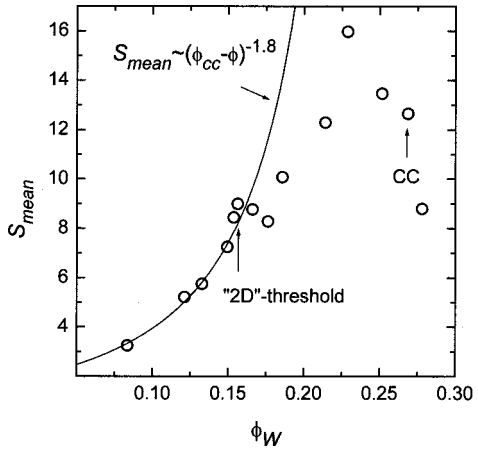

FIG. 6. Mean size of water clusters (excluded the largest cluster) versus volume fraction of water (circles). Below the percolation threshold S_{mean} follows a power law predicted by percolation theory with exponent $\gamma = 1.8$ (solid curve) if the composition of the organic-rich phase at coexistence is taken as a percolation threshold.

sizes $14 < s < 50$ the cluster distribution is consistent with a critical power law $n(s) \sim s^{-\tau}$ with an exponent $\tau \cong 2.2$. When the water concentration exceeds the threshold value, a specific ''hump'' appears at large cluster size [Fig. 4(c)], a feature usually related to the crossing of the percolation threshold. However, the range of validity of the critical law is much narrower than it is commonly found in continuous systems.[11] Moreover, the other cluster properties do not follow the critical percolation behavior. For, example, the fractal dimension of the infinite clusters at the threshold is found at about $d_f \cong 1.9$, significantly below the critical value $d_f \cong 2.5$ observed in 3D lattices and close to the value $d_f \cong 91/48$, predicted for 2D percolation (see Fig. 5). The 3D value of d_f itself is reached just at the organic-rich branch of the coexistence curve. Concerning the mean cluster size S_{mean}, it shows a local maximum at the percolation threshold and continues to increase with increasing water concentration (Fig. 6).

Accordingly one can conclude that percolation of water in the organic-rich phase between $w_W = 0.183$ and $w_{W,\mathrm{CC}} = 0.298$ is essentially a 2D percolation. The average number of H bonds per water molecule n_{H} at this threshold is $n_{\mathrm{H}} = 1.80$ (see Table I) that is close to the bond percolation threshold for pure water, observed when varying the H-bond definition [$n_{\mathrm{H}} = 1.55$ (Ref. 34)]. For comparison, near the water critical point $n_{\mathrm{H}} = 1.6$.[35]

The 3D percolation threshold of water occurs right at the organic-rich branch of the coexistence curve ($w_{W,\mathrm{CC}} = 0.298$), where the fractal dimension of the infinite cluster achieves the 3D value $d_f = 2.53$ (Fig. 5). At this concentration the cluster size distribution obeys a power law behavior in a wide range of cluster sizes $1 < s < 80$ [Fig. 7(b)]. For lower concentrations a positive deviation from the power law is observed in the cluster size range below the hump related to ''infinite'' clusters [Fig. 7(a)]. For the water concentration just inside the two-phase region a negative deviation from the power law is noticeable before the hump [Fig. 7(c)]. The pronounced decrease of the mean cluster size S_{mean} before the water content achieves $w_{W,\mathrm{CC}}$ (Fig. 6), also indicates a percolation threshold in this concentration range. Besides, below the percolation threshold the increase of the mean cluster size is consistent with the power law $S_{\mathrm{mean}} \sim (p_{\mathrm{CC}-p})^{-\gamma}$ with the exponent $\gamma = 1.8$ of geometrical percolation,[19] where p_{CC} is the value of the concentration variable p on the coexistence curve. (See Fig. 6, where the volume fraction of water is used as a concentration variable.)

In simple models the percolation threshold is very sensitive to the criteria of connectivity between molecules.

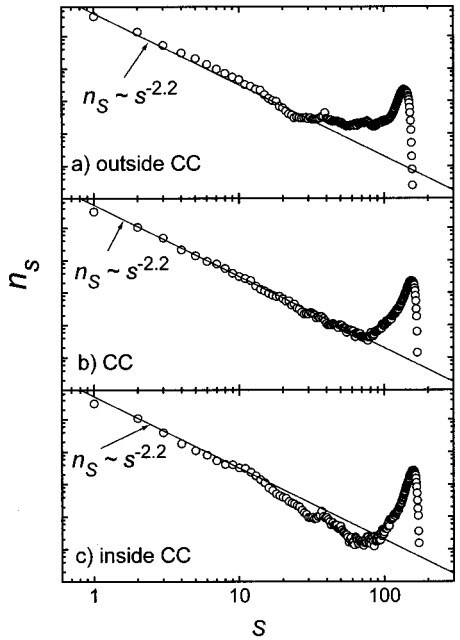

FIG. 7. Size distribution of water clusters in three solutions close to the organic-rich branch of the coexistence curve CC: (a) $w_W = 0.280$ (one-phase region outside the immiscibility gap), (b) $w_{W,\mathrm{CC}} = 0.298$ (organic-rich phase at coexistence), and (c) $w_W = 0.309$ (concentration inside the immiscibility gap, probably in the metastable region). Scaling law, predicted theoretically at the percolation threshold, is shown by lines.

Downloaded 07 Oct 2004 to 129.217.216.20. Redistribution subject to AIP license or copyright, see http://jcp.aip.org/jcp/copyright.jsp

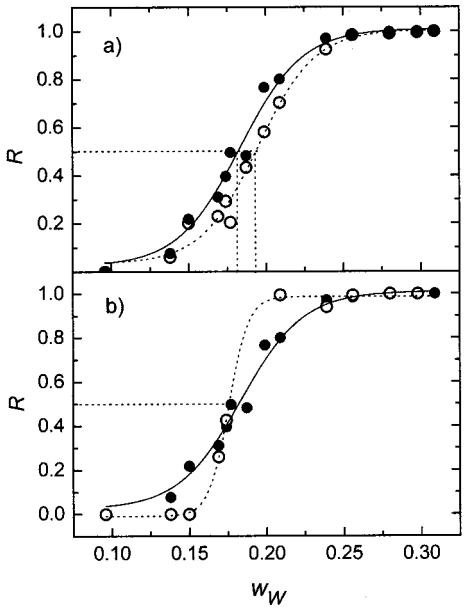

FIG. 8. Probability R to find an infinite cluster as function of the mass fraction of water w_W. (a) With the energetic criterion for water connectivity $U_W = -2.6$ kcal mol^{-1} (solid circles, solid curve) and $U_W = -2.8$ kcal mol^{-1} (open circles, dotted curve). The variation from -2.6 to -2.8 increases the percolation threshold from $w_W = 0.183$ to $w_W = 0.195$ (vertical dotted lines). (b) Influence of the size of the simulation box $L = 26.5$ A (solid circles, solid curve) and $L = 53$ A (open circles, dotted curve). No significant shift of the percolation threshold is visible.

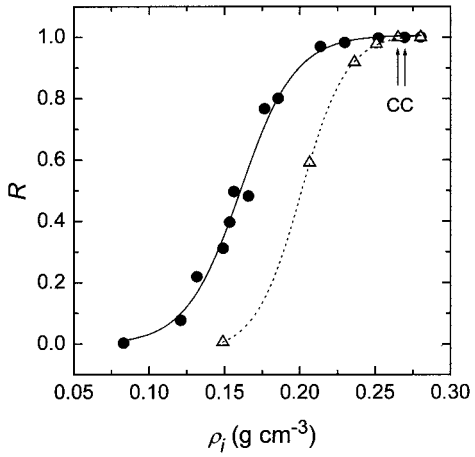

FIG. 9. Probability R to find an infinite cluster of water (solid circles, solid curve) or THF (triangles, dotted curve) as a function of partial mass density ρ_i of water or THF, respectively.

This is why these criteria are still an area of discussions.[11] This is not the case for water at ambient conditions, where the chosen distance and energy criteria for the hydrogen bonds can be fixed within a narrow range. Nevertheless, we have checked the influence of the connectivity criteria on the percolation threshold and other percolation properties. Figure 8(a) shows the change of the probability R to find an infinite cluster if the criterion for pair energy $U_W = -2.8$ kcal mol^{-1} is chosen instead of $U_W = -2.6$ kcal mol^{-1} used above. The strengthening of the energetic criterion results in a shift of the percolation threshold of about 6% and a decrease of 0.06 on the average number of H bonds per molecule in all investigated solutions.

In order to check the finite-size effect on the location of the percolation threshold we performed simulations with 8 times more molecules at the same concentrations. We observe no significant shift of the percolation threshold [see Fig. 8(b)], determined as the probability $R = 0.5$ to find an infinite cluster, although the concentration dependence of R becomes steeper.

In summary the formation of an infinite water network with increasing water concentration in aqueous solution takes place in two steps. The first step is attributed to a quasi-2D percolation that occurs at low water concentrations far away from the coexistence curve. This step is characterized by the appearance of infinite clusters with fractal dimension corresponding to the 2D percolation, the presence of a characteristic hump on the cluster size distribution and by a local maximum of the mean cluster size (susceptibility) at the percolation threshold. Onset of the true 3D percolation is observed on the organic-rich branch of the coexistence curve, where the fractal dimension of the infinite cluster reaches the theoretical 3D value $d_f \cong 2.5$ and where the cluster distribution follows a power law (with $\tau \cong 2.2$) over a wide range of cluster sizes.

We have also done an analysis of water clustering at higher temperatures, namely $T = 350$ K and $T = 375$ K. The interval of concentration between the quasi-2D percolation threshold and the coexistence curve is found similar to the one observed at $T = 325$ K. The fractal dimension of the infinite clusters at the coexistence curve is found to be $d_f \cong 2.5$ for $T = 350$ K and $d_f \cong 2.7$ for $T = 375$ K. The cluster size distribution shows a power law behavior at the concentration of coexistence on the organic-rich branch of the coexistence curve at $T = 350$, and at a slightly lower water concentration at $T = 375$ K. This small deviation of the 3D percolation threshold at higher temperatures could probably be corrected by readjusting the connectivity criteria, e.g., taking into consideration the kinetic energy contribution to the binding energy.

To compare the percolation process of water molecules with the behavior of the organic component, which consists of more simple particles, we performed also a cluster analysis of the THF molecules. The distance-energy criterion for THF connectivity includes a distance cutoff $R_{\mathrm{THF}} = 7.5$ A and an energy cutoff $U_{\mathrm{THF}} = -0.5$ kcal mol^{-1}, found from the pair correlation function between centers of the THF molecules and from the distribution of the THF–THF pair energies, respectively. The main results of the percolation analysis for 6 mixtures are given in Table I (mixtures 15–20). The probabilities to find an infinite THF cluster are shown in Fig. 9 as a function of THF density. A percolation threshold for the THF molecules (at $\rho_{\mathrm{THF}} = 0.201$ g cm^{-3}, Fig. 9, which corresponds to $w_{\mathrm{THF}} = 0.207$, as indicated in Fig. 1; $x_{\mathrm{THF}} = 0.061$; $\varphi_{\mathrm{THF}} = 0.232$) is observed below the THF concentration of the water-rich phase (at $\rho_{\mathrm{THF,CC}} = 0.265$ g cm^{-3}, Fig. 9; $w_{\mathrm{THF,CC}} = 0.275$, Fig. 1; $x_{\mathrm{THF,CC}} = 0.087$; $\varphi_{\mathrm{THF,CC}} = 0.305$). The THF percolation starts approximately at 24% in volume fraction of THF, normalized to the maximum packing fraction. This latter value is in reasonable agreement

Downloaded 07 Oct 2004 to 129.217.216.20. Redistribution subject to AIP license or copyright, see http://jcp.aip.org/jcp/copyright.jsp

with the critical volume fraction obtained for interacting spheres.[5,62] However, the maximum of the mean cluster size and the occurrence of the 3D value for the fractal dimension of the infinite cluster are observed closer to the coexistence curve than the 50% probability R to find an infinite cluster. In general, the results for THF percolation in aqueous solution are less reliable than those for water percolation due to several reasons. The THF molecules are quite large and their mobility in solution is lower than that of water. Therefore, a correct sampling of cluster configurations becomes difficult at low THF concentrations. The connectivity criteria for THF are more ambiguous than for water due to weaker and more isotropic interactions. Moreover, these criteria for THF clustering are more sensitive to the thermodynamic conditions because the pair interactions are of the order of k_BT. Finally notice that investigating THF percolation in water-rich solutions needs thousands of water molecules in the simulation box (see Table I), a requirement that makes the computer study of THF percolation extremely time consuming.

In view of shortcomings of the above-mentioned percolation analysis we can only conclude that percolation of the organic molecules occurs at a THF concentration close to or slightly below the water-rich branch of the coexistence curve.

IV. CONCLUSIONS

The percolation of water in an aqueous mixture (THF + water) is observed in a wide concentration range on both sides of the liquid–liquid coexistence curve. It proceeds in two steps. In a first step an infinite cluster with fractal dimension close to the 2D percolation value appears in the system at a water concentration $x_W \approx 0.53$, i.e., far below the concentration of unmixing. This conclusion agrees with an assumption made many years ago[63] about the presence of 2D water surfaces in THF+water mixtures around $x_W \approx 0.5$. Besides, a 2D percolation threshold of water in hydrated proteins was observed by a sharp increase of the protonic conductivity.[64] At this threshold water molecules adsorbed on the surface of the protein form a network along which protons can be transferred. It's appearance was reported at water concentrations from $w_W = 0.08$ to 0.15 for various proteins, which is comparable with $w_W \approx 0.18$ obtained in our study and less than monolayer coverage. It was established that a 2D percolation threshold of water coincides with the onset of water-induced functionality of biological molecules, for example, enzymatic activity of proteins.[64]

The occurrence of 3D percolation is observed directly at the organic-rich branch of the coexistence curve. At this water concentration the fractal dimension of an infinite cluster reaches the 3D value $d_f \cong 2.5$ and the clusters size distribution follows a power law with the corresponding critical exponent $\tau \cong 2.2$.

The present study suggests a new method to locate the liquid–liquid coexistence curve in aqueous solutions based on an analysis of clustering. The first clue is given by the critical fractal dimension of infinite clusters $d_f \cong 2.5$ (Fig. 5, Table I) and the second one is a log–log analysis of the cluster size distribution (Fig. 7). The latter distribution seems to be a very sensitive indicator of the crossing of the coexistence curve. Thus a negative deviation of the cluster size distribution from the power law in the cluster size region just below the hump [Fig. 7(c)] coincides with the entering into the metastable region inside the coexistence curve.

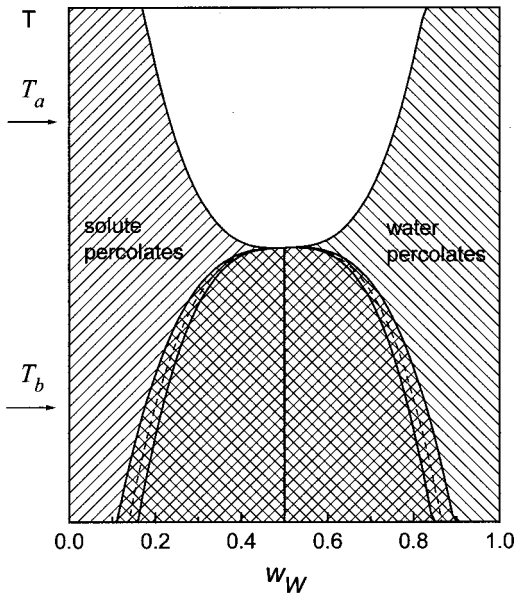

FIG. 10. Schematic liquid–liquid coexistence curve of an aqueous solution (dashed line) and location of the percolation thresholds of water and solute molecules (solid lines). Simultaneous percolation of both components occurs in the double-hatched region, which coincides approximately with the coexistence curve (the solution develops an immiscibility gap at $T = T_b$). In the totally miscible solution at $T = T_a$ the percolation regions of the two components do not overlap. At higher temperatures both percolation lines will reach the liquid–vapor critical points of the pure components.

The percolation threshold of THF is observed on the water-rich side of the region of immiscibility, very close to the water-rich branch of the coexistence curve. So, the immiscibility gap of the investigated aqueous solution corresponds to the concentration interval where both water and organic solute are above their respective percolation threshold. These findings lead to the somewhat paradoxical hypothesis, that for completely miscible aqueous solutions (no immiscibility gap) the percolation regions of the two components do not overlap. Combining our findings for subcritical temperatures with observations of the percolation behavior in supercritical systems[4,10,18] we construct the schematic Fig. 10, which indicates the location of the percolation threshold for both components. In line with the above hypothesis, T_a corresponds to completely miscible solution, while at T_b an immiscibility gap is opening. Below we give some additional arguments to support this conclusion and discuss its correspondence with available experimental results.

As evoked earlier, the strengthening of THF–water cross interactions causes a strong shrinking of the immiscibility region.[49] This is accompanied by a decrease of water–water hydrogen bonding and by a shift of the water percolation threshold towards higher water concentration. In particular, a strengthening of the Coulombic THF–water cross interactions by a factor of 2.0 instead of a factor 1.2 decreases the average number of water–water H-bonds per molecule by 0.7 and the 2D percolation threshold shifts from 0.19 to 0.30

Downloaded 07 Oct 2004 to 129.217.216.20. Redistribution subject to AIP license or copyright, see http://jcp.aip.org/jcp/copyright.jsp

mass fraction of water. Conversely, a weakening of THF–water cross interactions causes a strong extension of the immiscibility region[49] and an increase of water–water hydrogen bonding.[57]

Our results agree with the experimentally observed evolution of the immiscibility gap upon deuteration of THF or water.[51,52] It is reasonable, that the replacement of the protons of THF by deuterons effects mainly the THF–water interaction. Due to its strengthening, the water percolation threshold shifts to higher water concentrations and causes a shrinkage of the immiscibility gap. Deuteration of water strengthens both water–water and THF–water interactions, but this effect will be more significant for the water–water interactions, hence, one could expect the water percolation threshold to shift to a lower content and thus lead to an extension of the immiscibility gap.

The idea, that for completely miscible aqueous solutions the percolation regions of the two components do not overlap, is also supported by available experimental results. In completely miscible mixtures of water and 1,4-dioxane the hydrogen-bonded water network is observed only below 0.1 mole fraction of dioxane, while bulklike dioxane clusters are found only above 0.3 mole fraction.[37] Similar results were obtained for completely miscible alcohol–water mixtures.[43] Another example is given by the acetonitrile+water mixture, where a liquid–liquid phase separation is observed at some salt concentration. This is interpreted as due to an increase of water–water hydrogen bonds.[42]

The percolation behavior of the components in a binary mixture in relation to the region of immiscibility seems to be very similar to water-oil-surfactant microemulsions, which possess two micellar and a bicontinuous phase. Experimental studies of the water and oil percolation in such systems showed that the bicontinuous phase corresponds to the concentration range where both oil and water are above their percolation thresholds.[65] When only one component percolates the system shows micellar structure. The volume fractions of water and oil at their percolation thresholds were found near 20% which is quite close to our results for water and THF. The presence of the percolation clusters of both components results in a bicontinuous microemulsion, which has to be stabilized by surfactant, whereas macroscopic phase separation is observed in the binary mixtures without surfactant.

Note also, that the idea to connect percolation phenomena with liquid–liquid immiscibility in aqueous solutions is also explored in a recent paper,[66] where the region of immiscibility is attributed to the percolation of ''solute-rich clusters.''

Finally, we would like to mention that it may be reasonable to expect the percolation threshold to coincide not with the coexistence curve, but the spinodal line.[21] However, there is no unambiguous way to locate the spinodal line. It is possible, that in aqueous solutions the spinodal is quite close to the liquid–liquid coexistence curve (see Ref. 67, for example). Thus, we cannot exclude that the percolation thresholds for both components in THF+water mixture coincide with the spinodal lines within the accuracy of present simulations.

Summarizing, we present results which suggest that cluster analysis may be a useful way of locating liquid–liquid coexistence curves. However, further work is needed to establish a more general and firm connection between percolation transition and phase separation.

ACKNOWLEDGMENTS

We thank Professor J. Meunier for providing his paper prior to publication. This work was supported by the Ministerium fur Wissenschaft und Forschung des Landes Nordrhein–Westfalen and by DFG Forschergruppe 436.

[1] J. E. Mayer, J. Chem. Phys. **5**, 67 (1937).
[2] A. Coniglio, Nucl. Phys. A **681**, 451c (2001); J. Phys.: Condens. Matter **13**, 9039 (2001).
[3] M. E. Fisher, Physics **3**, 25 (1967).
[4] A. Coniglio and W. Klein, J. Phys. A **13**, 2775 (1980).
[5] S. A. Safran, I. Webman, and G. S. Grest, Phys. Rev. A **32**, 506 (1985).
[6] J. Xu and G. Stell, J. Chem. Phys. **89**, 1101 (1988).
[7] Y. C. Chiew, J. Chem. Phys. **110**, 10482 (1999).
[8] J. Kertesz, Physica A **161**, 58 (1989).
[9] H. Satz, hep-lat/0110013 2001.
[10] N. Yoshii and S. Okazaki, J. Chem. Phys. **107**, 2020 (1997).
[11] X. Campi, H. Krivine, and N. Sator, Nucl. Phys. A **681**, 458c (2001).
[12] N. Yoshii, H. Yoshie, S. Miura, and S. Okazaki, J. Chem. Phys. **109**, 4873 (1998).
[13] N. Yoshii, S. Miura, and S. Okazaki, Bull. Chem. Soc. Jpn. **72**, 151 (1999).
[14] R. D. Mountain, J. Chem. Phys. **110**, 2109 (1999).
[15] J. Marti, J. Chem. Phys. **110**, 6876 (1999).
[16] M. Boero, K. Terakura, T. Ikeshoji, C. C. Liew, and M. Parinello, Phys. Rev. Lett. **85**, 3245 (2000).
[17] A. G. Kalinichev and S. V. Churakov, Fluid Phase Equilib. **183–184**, 271 (2001).
[18] X. Campi, H. Krivine, and A. Puente, Physica A **262**, 328 (1999).
[19] D. Stauffer, *Introduction to Percolation Theory* (Taylor & Francis, London, 1985).
[20] N. Jan, Physica A **266**, 72 (1999).
[21] W. Klein, Phys. Rev. Lett. **47**, 1569 (1981); **65**, 1462 (1990).
[22] C. P. Schioppa, F. Sciortino, and P. Tartaglia, Phys. Rev. E **57**, 3797 (1998).
[23] K. Binder, Phys. Rev. B **8**, 3423 (1973).
[24] D. W. Heermann, Z. Phys. B: Condens. Matter **55**, 309 (1984).
[25] D. W. Heermann, K. Binder, and S. Hayward, Philos. Mag. B **56**, 843 (1987); S. Hayward, D. W. Heermann, and K. Binder, J. Stat. Phys. **49**, 1053 (1987).
[26] J. Richert and P. Wagner, Phys. Rep. **350**, 3 (2001).
[27] J. B. Elliott *et al*. Phys. Rev. C **62**, 064603 (2000).
[28] J. Pan, S. Das Gupta, and M. Grant, Phys. Rev. Lett. **80**, 1182 (1998); J. Pan and S. Das Gupta, Phys. Rev. C **57**, 1839 (1998).
[29] J. Borg, I. N. Mishustin, and J. P. Bondorf, Phys. Lett. B **470**, 13 (1999).
[30] F. Gulminelli, Ph. Chomaz, and V. Duflot, Europhys. Lett. **50**, 434 (2000).
[31] J. M. Carmona, J. Richert, and A. Tarancon, Nucl. Phys. A **643**, 115 (1998); J. M. Carmona, J. Richert, and P. Wagner, Eur. Phys. J. A **11**, 87 (2001).
[32] H. E. Stanley and J. Teixeira, J. Chem. Phys. **73**, 3404 (1980).
[33] A. Geiger, F. H. Stillinger, and A. Rahman, J. Chem. Phys. **70**, 4185 (1979); A. Geiger and H. E. Stanley, Phys. Rev. Lett. **49**, 1895 (1982).
[34] R. L. Blumberg, H. E. Stanley, A. Geiger, and P. Mausbach, J. Chem. Phys. **80**, 5230 (1984).
[35] Y. Guissani and B. Guillot, J. Chem. Phys. **98**, 8221 (1993).
[36] V. I. Korsunskii and Yu. I. Naberukhin, J. Struct. Chem. **18**, 470 (1977).
[37] T. Takamuku, A. Yamaguchi, M. Tabata, N. Nishi, K. Yoshida, H. Wakita, and T. Yamaguchi, J. Mol. Liq. **83**, 163 (1999).
[38] T. Takamuku, A. Yamaguchi, D. Matsuo, M. Tabata, T. Yamaguchi, T. Otomo, and T. Adachi, J. Phys. Chem. B **105**, 10101 (2001).
[39] T. Mashimo, N. Miura, T. Umehara, S. Yagira, and K. Higasi, J. Chem. Phys. **96**, 6358 (1992).
[40] Y. Tominaga and S. M. Takeuchi, J. Chem. Phys. **104**, 7377 (1996).
[41] T. Takamuku, M. Tabata, A. Yamaguchi, J. Nishimoto, M. Kumamoto, H. Wakita, and T. Yamaguchi, J. Phys. Chem. B **102**, 8880 (1998).

Downloaded 07 Oct 2004 to 129.217.216.20. Redistribution subject to AIP license or copyright, see http://jcp.aip.org/jcp/copyright.jsp

[42] T. Takamuku, A. Yamaguchi, D. Matsuo *et al*. J. Phys. Chem. B **105**, 6326 (2001).
[43] (a) T. Sato, A. Chiba, and R. Nozaki, J. Chem. Phys. **112**, 2924 (2000); (b) **110**, 2508 (1999); (c) **113**, 9748 (2000).
[44] P. A. Brooksby and W. R. Fawcett, J. Phys. Chem. A **104**, 8307 (2000).
[45] Y. Koga, J. Phys. Chem. **100**, 5172 (1996).
[46] K. Zamura, A. Osaki, and Y. Koga, Phys. Chem. Chem. Phys. **1**, 121 (1999).
[47] D. Bonn, D. Ross, S. Hachem, S. Gridel, and J. Meunier, Europhys. Lett. **58**, 74 (2002).
[48] D. B. Bergman and A. Laaksonen, Phys. Rev. E **58**, 4706 (1998); C. J. Roberts and P. G. Debenedetti, J. Phys. Chem. B **103**, 7308 (1999).
[49] I. Brovchenko and B. Guillot, Fluid Phase Equilib. **183–184**, 311 (2001).
[50] J. Matous, J. Hrncirik, J. P. Novak, and J. Sobr, Collect. Czech. Chem. Commun. **35**, 1904 (1970); P. Lejcek, J. Matous, J. P. Novak, and J. Pick, J. Chem. Thermodyn. **7**, 972 (1975).
[51] A. Oleinikova and H. Weingärtner, Chem. Phys. Lett. **319**, 119 (2000); Phys. Chem. Chem. Phys. **4**, 955 (2002).
[52] V. Balevicius, N. Weiden, and A. Weiss, Ber. Bunsenges. Phys. Chem. **98**, 785 (1994).
[53] I. Brovchenko and A. Oleinikova, J. Chem. Phys. **106**, 7756 (1997).
[54] I. Papai and G. Jancso, J. Phys. Chem. A **104**, 2132 (2000).
[55] W. L. Jorgensen, J. Chandrasekhar, and J. D. Madura, J. Chem. Phys. **79**, 926 (1983).
[56] J. Chandrasekhar and W. L. Jorgensen, J. Chem. Phys. **77**, 5073 (1982).
[57] L. C. Gomide Freitas and J. M. Marques Cordeiro, J. Mol. Struct. **335**, 189 (1995).
[58] P. J. Back and L. A. Woolf, J. Chem. Thermodyn. **30**, 353 (1998).
[59] A. Oleinikova (unpublished).
[60] T. M. Aminabhavi and B. Gopalakrishna, J. Chem. Eng. Data **40**, 856 (1995).
[61] S. J. Suresh and V. M. Naik, J. Chem. Phys. **113**, 9727 (2000).
[62] A. L. R. Bug, S. A. Safran, G. S. Grest, and I. Webman, Phys. Rev. Lett. **55**, 1896 (1985).
[63] D. N. Glew and H. Watts, Can. J. Chem. **51**, 1933 (1973).
[64] G. Careri, A. Giansanti, and J. A. Rupley, Phys. Rev. A **37**, 2703 (1988); F. Bruni, G. Careri, and A. C. Leopold, *ibid.* **40**, 2803 (1989); G. Careri and M. Peyrard, Cell Mol. Biol. (Paris) **47**, 745 (2001).
[65] M. Borkovec, H.-F. Eicke, H. Hammerich, and B. D. Gupta, J. Phys. Chem. **92**, 206 (1988).
[66] M. Misawa and K. Yoshida, J. Phys. Soc. Jpn. **69**, 3308 (2000).
[67] N. F. Bunkin, A. V. Lobeev, and G. A. Lyakhov, Phys. Usp. **40**, 1019 (1997).

Downloaded 07 Oct 2004 to 129.217.216.20. Redistribution subject to AIP license or copyright, see http://jcp.aip.org/jcp/copyright.jsp